Characterization of Contour Shapes Achievable with a MEMS Deformable Mirror

Yaopeng Zhou and Thomas Bifano
Manufacturing Engineering Department, Boston University
15 Saint Mary's Street, Brookline MA, 02446
ypzhou@bu.edu and tgb@bu.edu

ABSTRACT

An important consideration in the design of an adaptive optics controller is the range of physical shapes required by the DM to compensate the existing aberrations. Conversely, if the range of surface shapes achievable with a DM is known, its suitability for a particular AO application can be determined. In this paper, we characterize one MEMS DM that was recently developed for vision science applications. The device has 140 actuators supporting a continuous face sheet deformable mirror having 4mm square aperture. The total range of actuation is about 4µm, achieved using electrostatic actuation in an architecture that has been described previously. We incorporated the MEMS mirror into an adaptive optics (AO) testbed to measure its capacity to transform an initially planar wavefront into a wavefront having one of thirty-six orthogonal shapes corresponding to the first seven orders of Zerinke polynomials. The testbed included a superluminescent diode source emitting light with a wavelength 630nm, a MEMS DM, and a Shack Hartmann wavefront sensor (SHWS). The DM was positioned in a plane conjugate to the SHWS lenslets, using a pair of relay lenses. Wavefront slope measurements provided by the SHWS were used in an integral controller to regulate DM shape. The control software used the difference between the the wavefront measured by the SHWS and the desired (reference) wavefront as feedback for the DM. The DM is able to produce all 36 terms with a wavefront height root mean square (RMS) from 1.35µm for the lower order Zernike shapes to 0.2µm for the 7th order.

Key words: adaptive optics, deformable mirror

1. INTRODUCTION

The goal for an adaptive optics (AO) control system is to compensate for the imperfections of the optics, allowing imaging the target with higher resolution and sharper contrast. The deformable mirror (DM) is an enabling component in the AO system. DMs manufactured using thin film processes collectively known as microelectromechanical systems (MEMS) are finding increased use in recent years, due to their compact size, low cost, and low power consumption. Applications include astronomical imaging [1], microscopy [2] and vision science [3].

The achievable contour shape on the mirror surface quantifies the mirror's ability to reshape the wavefront in the optical system. In this work, we characterize one MEMS DM that was recently developed for vision science by Boston Micromachines Corporation of Watertown, MA, for this purpose.

In AO for vision science, the goal is to compensate for the imperfections of the optics of the eye, allowing *in vivo* images of unprecedented resolution and contrast. The defects in an optical system are quantified by the wavefront measurement, and compensated by the wavefront correction. Zernike polynomials have been widely used as a set of orthogonal wave functions to characterize eye aberration in the pupil plane. In this paper, we will display the achievable wave shape by the MEMS DM up the 7th order Zernike polynomial [4].

2. METHODS

The MEMS DM used in this work is produced by Boston University and Boston Micromachines Corporation. The DM includes 140 actuators and has 4.4mm clear aperture and good optical surface quality. Figure 1 shows Optical microphotograph of the MEMS DM and a drawing of the device concept.
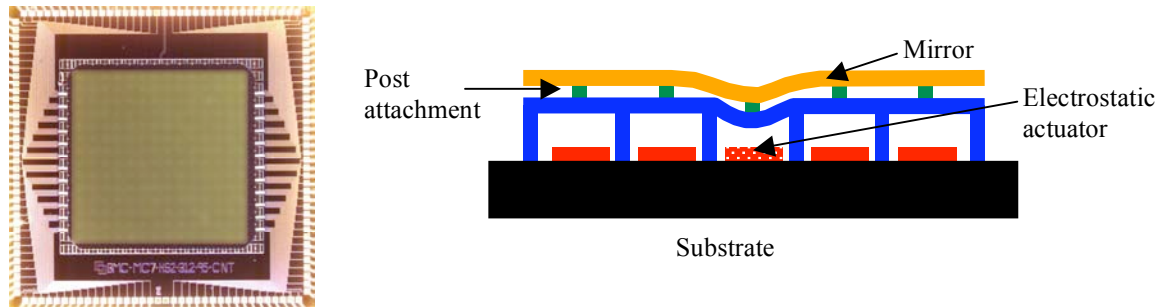

Figure 1. Optical microphotograph (left) and cross sectional schematic (right) of the BMC MEMS DM. The clear aperture of the mirror is 4.4mm. It is supported on an array of 12 x 12 electrostatic actuators on a 400μm square pitch. The four corner actuators are not used. Each actuator is connected to the continuous mirror membrane by a single post attachment. Actuators can pull the mirror toward the substrate by up to 4μm in response to an applied voltage. Each actuator is controlled independently.

The DM was incorporated into a simple adaptive optics (AO) testbed. The system is illuminated by a collimated beam formed by a superluminescent diode emitting light at a wavelength 630nm. The wavefront is measured using a Shack Hartmann wavefront sensor (SHWS), consisting of a lenslet array, a CCD camera, a frame grabber, and a custom developed software interface. The DM is located in an optical plane conjugate to the SHWS lenslet array. In the adaptive optics control loop, the wavefront measured by the SHWS is subtracted from a reference wavefront. The resulting error in wavefront is used as integral feedback to control the DM. In a calibration step, each actuator is deflected independently by a unit amount, and the resulting wavefront slope array is recorded. From a least-squares fit to this ensemble dataset, a reconstructor matrix is constructed to map the SHWS measurement to corresponding wavefront through a singular value decomposition technique. The control software then uses the wavefront error and a characteristic model of the mirror to determine the appropriate compensatory voltage to apply to each actuator in the DM.

The objective of the control algorithm in its simplest form is to move the deformable mirror actuators in a way that minimizes the wavefront error. The wavefront reference can correspond to any wavefront shape that is desired. A particularly interesting set of shapes that can be imposed on the wavefront are the Zernike polynomials, an orthogonal basis defined over a unit circle.
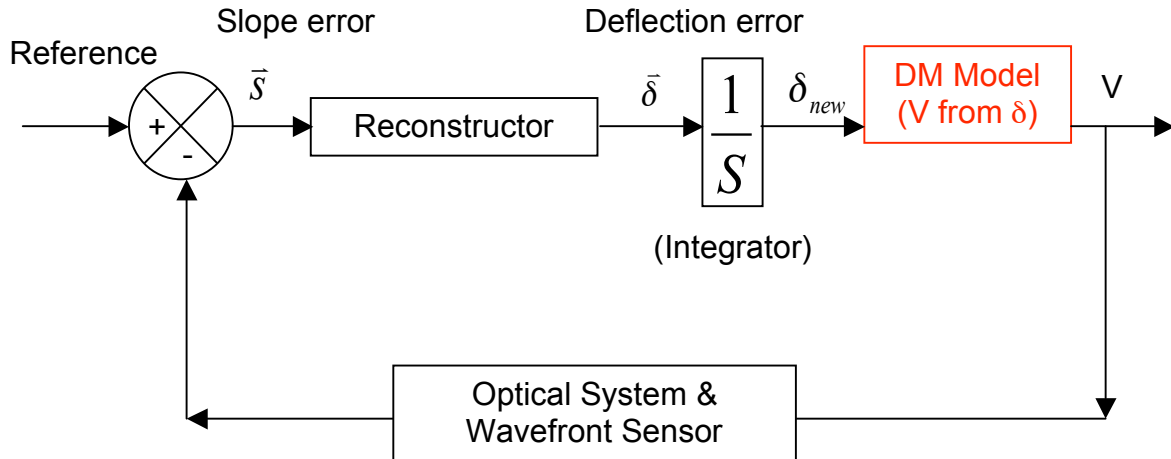
Reference   Slope error   Deflection error

$+$ $-$ $\bar{s}$ **Reconstructor** $\bar{\delta}$ $\dfrac{1}{S}$ δ_{new} **DM Model (V from δ)** V

(Integrator)

Optical System & Wavefront Sensor

Figure 2. AO closed loop block diagram. The control loop uses simple feedback based on the vectors $\bar{\delta}$ and $\bar{s}$ representing the actuator displacement inputs and measured SHWS slopes respectively.

The range of wavefronts controllable by the DM is limited by the actuator stroke and resolution, the number and distribution of actuators in the DM, and the model used to convert the desired mirror deflection to appropriate control signals for the DM. Because mechanical coupling exists among actuators through the mirror, deflection of an actuator depends (nonlinearly) on both the voltage applied to that actuator and the relative deflection of its near neighbors. For example, when the DM is deformed by energizing a single actuator, mechanical coupling forces on nearby actuators result in their simultaneous deflection, even though they are not being energized with an applied voltage. For the DM geometry used in this work, such mechanical coupling results in a deflection of nearest neighbors by about 15% of the amount that the energized actuator is deflected.

Figure 3 is a schematic of the electromechanical equilibrium state that characterizes each DM post attachment. The Figure shows cross sections of five actuators with different applied voltages. At each post, equilibrium can be found among three forces: the electrostatic applied force, the actuator membrane restoring force, and the force influence of the mirror. These three forces can be estimated using well-known models for parallel plate electrostatic attraction, elastic beam bending, and thin plate bending and stretching.

F_{Mirror}

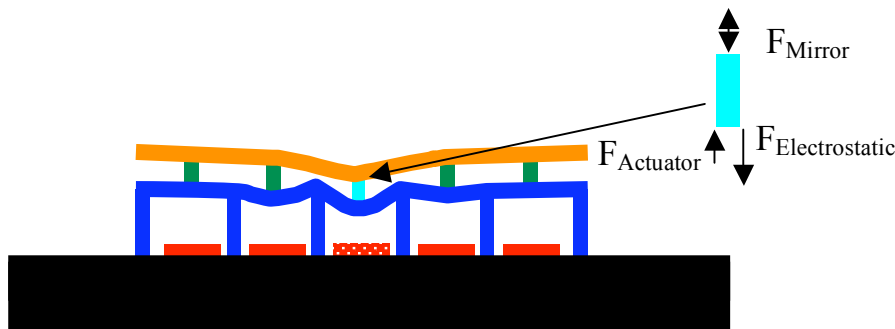$F_{Actuator}$ $F_{Electrostatic}$

Figure 3. Schematic cross section of five actuators and a mirror. Three components of force at each actuator post contribute to the local equilibrium displacement of the mirror.

To develop a suitable model to map an array of desired DM actuator deflections to an array of input voltages, the DMs were first characterize by empirical measurements made using an interferometric microscope. A single actuator was subjected to a range of applied voltages, while all other actuators were unenergized (i.e. electrically held at 0V) Deflection, measured on the mirror at a position directly above the center of the energized actuator, was found to vary approximately quadratically with applied voltage, as shown in Figure 4.
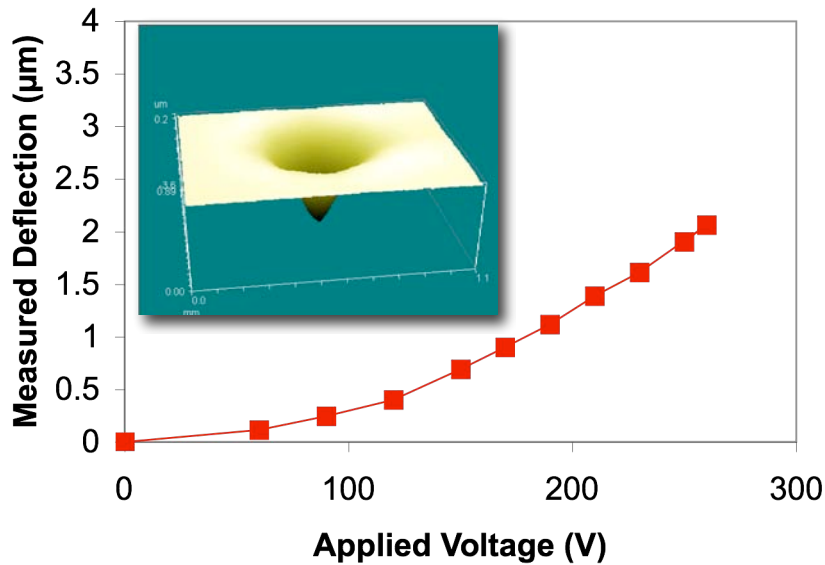

Figure 4. DM deflection measured at a location above a single actuator that was energized while all other actuators remained unenergized. A second order curve was fit to the measured data. Measurement resolution is about 25nm. All interior actuators in the DM have been shown to behave comparably. Edge and corner actuators achieve higher deflection for comparable voltage, but also respond quadratically to applied voltage, No hysteresis is expected or observed, and repeatability of ~2nm has been reported for these DMs when they were measured using a more precise characterization tool.

This voltage-deflection relationship was measured for one actuator, while all other actuators in the DM were unenergized. In this case, the initial state (voltage =0) is one in which the mirror exerts no force on the actuator being measured, because all neighboring actuators are at the same deflection.

The maximum local wavefront slope S that can be produced by the MEMS DM can be approximated by twice the ratio of the maximum deflection to the spacing between two actuators D, where the factor of two accounts for the fact that the wavefront is reflected from the deformed DM:

$$S = 2\delta/D \qquad\qquad \text{Equation 1}$$

For the DM used in this work, the maximum wavefront slope S is approximately 18milliradians.

Next, the voltage-deflection relation was measured for the same actuator, but this time all *other* actuators in the array were energized uniformly, achieving a nominal deflection of the mirror. In this case, the initial state (voltage =0) is one in which the mirror exerts a downward force on the actuator being measured, because all neighboring actuators are initially deflected. The resulting family of measured curves is depicted in Figure 4.
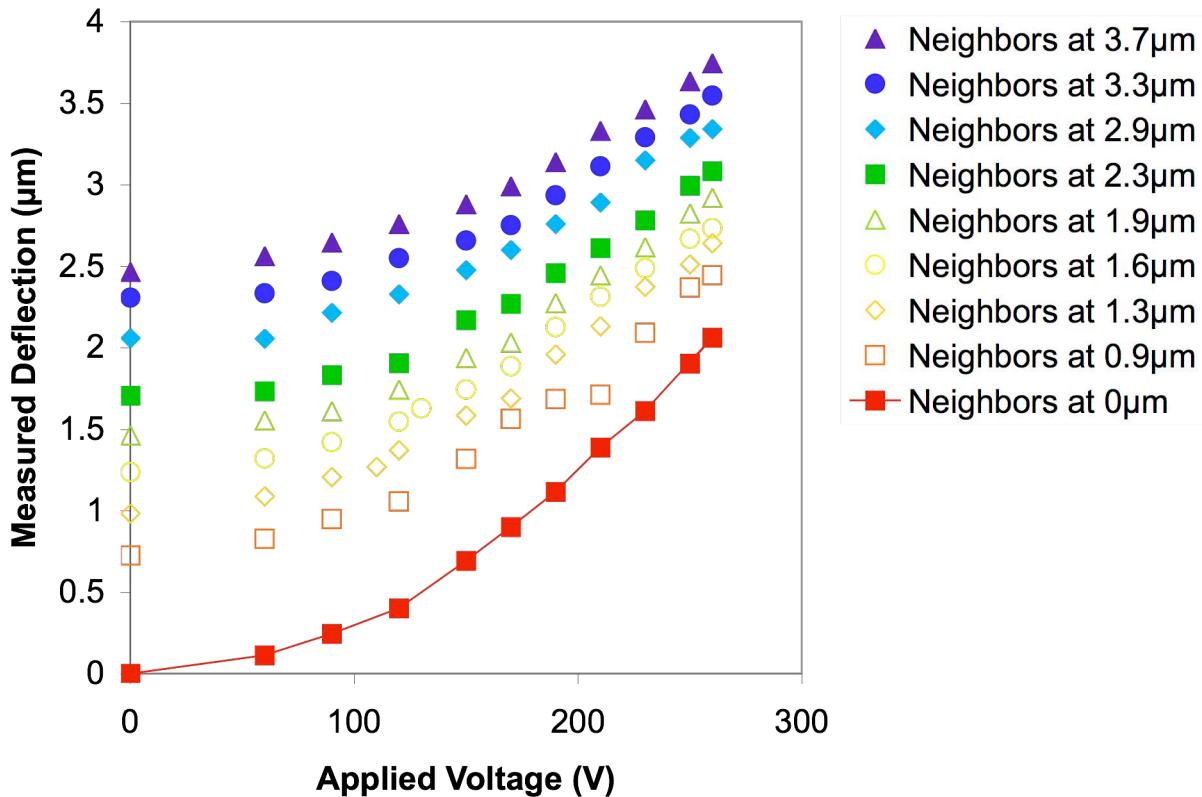
Figure 5. Voltage versus deflection for a single actuator when all other actuators are energized uniformly by a fixed amount. Each curve corresponds to a different nominal deflection of all other actuators, ranging from 0.0μm to 3.7μm. For any voltage, the deflection of the measured actuator increases with the nominal deflection of its neighbors. Note that the peak deflection is about 3.7μm for this DM at 260V, with all neighboring actuators similarly energized.

3. RESULTS

In a closed-loop control experiment, individual Zernike polynomials of varying amplitude were sequentially imposed as the controller reference (i.e. the target wavefront shape). The control loop was used to drive the DM to a desired shape using feedback from the SHWS. Figure 6 shows the measured shape of the second order to seventh order Zernike polynomials made by the DM subject to this closed loop control using these reference shapes. Table 1 shows the summary of the desired root mean square (RMS), achieved RMS, achieved Peak-Valley (PV) value and the residual wavefront error for each Zernike terms imposed on the DM. For higher orders, successively smaller amplitudes of Zernike polynomial were specified, to maintain approximately constant residual error. The maximum RMS value on the wavefront is limited by the actuator stroke, the inter-actuator coupling, the fitting error in the voltage to deflection map, and the wavefront slope-to-deflection reconstructor. Of these factors, the first two correspond to physical limitations of the DM, while the latter two correspond to limitations of the DM model.

In all cases, the error was limited to100nm RMS, corresponding to a Strehl ratio of 0.4 for an illumination wavelength of 650nm. If this criterion were relaxed, larger amplitudes would be possible for each Zernike shape.

It is important to note that the maximum amplitudes achieved in this experiment are limited both by the mirror and by the controller, and it is expected that these values will increase as the controller and DM model are improved. To illustrate this point, the controller was run using two alternative models of the DM, using a focus-term (Z4) of 0.5µm RMS amplitude as the controller reference. The two alternative models of the DM used in the controller are distinguished by their consideration of the coupling coefficient between actuators. In the model with coupling, the data plotted in Figure 5 was fit by a four-term model fitting the family of curves measured empirically. These curves specifically take into account the zeroth-order coupling between actuators. In the model without coupling, the voltage deflection behavior of an actuator when all neighboring actuators were similarly energized was measured, and fit with a second order least squares approximation. In this case, coupling among actuators is not captured by the empirical model. When used in the controller under identical conditions, the controller that mapped required displacement to applied voltage using the model with coupling was both faster to converge, and exhibited less error in steady state.
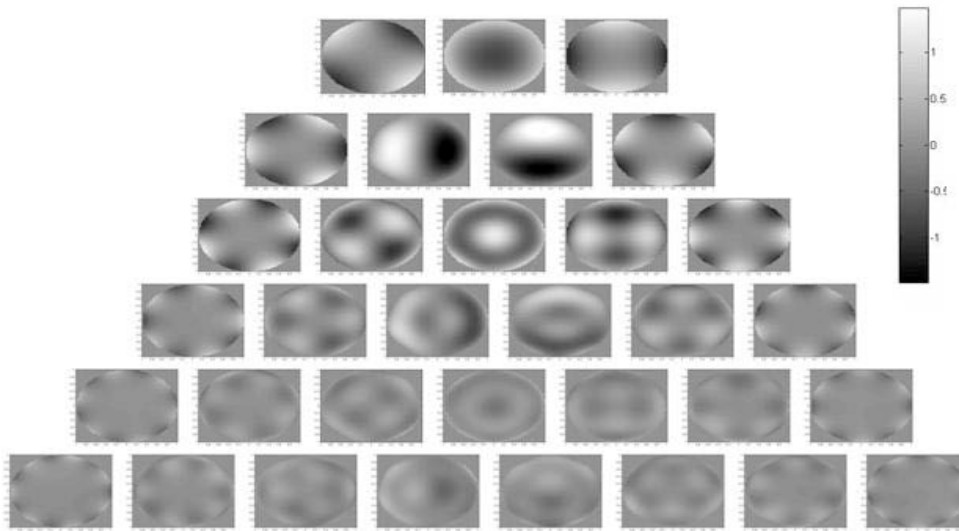

Figure 6. Measured contour maps of the final state of the wavefront sensor in closed-loop control experiments imposing 2rd to 7th order Zernike polynomials on the DM.

Zernike coefficient index (ANSI standard)	Description	Target RMS (µm)	Achieved RMS (µm)	Achieved Peak-Valley (µm)	Residual RMS error (µm)
3	Astigmatism	1.1	0.991	4.621	0.097
4	Defocus	1.35	1.273	4.505	0.103
5	Astigmatism	1.25	1.162	5.343	0.101
6	Trefoil	1	0.918	5.212	0.096
7	Coma	1	1.0476	6.18	0.1
8	Coma	1.1	1.0514	5.689	0.101
9	Trefoil	0.95	0.877	4.941	0.093
10		0.8	0.728	4.321	0.095
11		0.4	0.486	1.912	0.088
12	Spherical	0.7	0.695	2.69	0.099

13	0.5	0.523	2.584	0.103
14	0.75	0.672	3.932	0.1
15	0.65	0.574	4.258	0.099
16	0.4	0.38	2.25	0.087
17	0.4	0.389	3.019	0.09
18	0.4	0.366	2.556	0.086
19	0.4	0.376	2.399	0.091
20	0.7	0.624	4.47	0.099
21	0.45	0.379	3.229	0.079
22	0.3	0.242	1.812	0.076
23	0.2	0.157	1.056	0.1
24	0.3	0.234	1.697	0.095
25	0.3	0.238	1.708	0.1
26	0.3	0.241	1.822	0.089
27	0.5	0.421	3.508	0.088
28	0.4	0.307	2.539	0.099
29	0.25	0.184	1.714	0.09
30	0.2	0.142	1.414	0.084
31	0.2	0.125	1.0827	0.0954
32	0.2	0.135	1.22	0.092
33	0.2	0.145	1.409	0.095
34	0.25	0.189	1.639	0.081
35	0.4	0.32	2.725	0.0863

Table 1. Desired root mean square (RMS), achieved RMS, achieved Peak-Valley value and the residual wavefront error for each Zernike terms imposed on the DM.
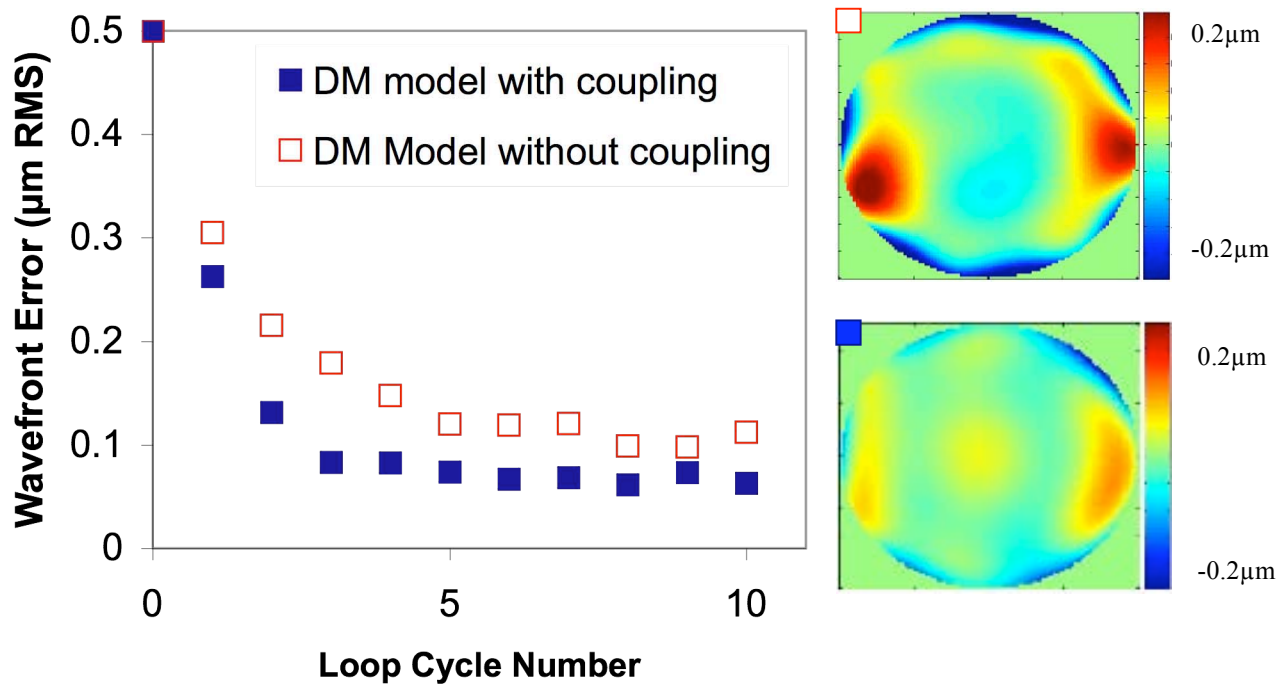
Figure 7: Results from control loop correcting a 0.5μm imposed focus error using two alternative models of the DM to convert from desired displacement to voltage applied to the array. One that takes into account the zeroth-order interactuator mechanical coupling, and one that ignores that coupling. The coupled model, as expected, provides faster convergence. The coupled model also converged to a steady state with smaller RMS error int he wavefront. At right is the measured contour map after the tenth cycle of the closed loop control, illustrating the difference in steady-state error achieved using these alternative models of the DM.

4. CONCLUSION

A MEMS DM was used to successfully produce a set of Zernike polynomial wavefront including all of the first 35 terms, through the seventh order. The DM was characterized to find its maximum stroke and maximum slope. A closed loop system was built to control the mirror to achieve the desired shape.

[1] Bifano, T. G., Perreault, J., Mali, R. K., and Horenstein, M. N., "Microelectromechanical Deformable Mirrors," Journal of Selected Topics in Quantum Electronics, [5], pp. 83-90, 1999

[2] M. J. Booth, M. A. A. Neil, R. Juskaitis, and T. Wilson, "Adaptive aberration correction in a confocal microscope," PNAS 99, 9, 5788-5792 (2002).

[3] Doble, N. and Williams, D.R.,"The application of MEMS technology for adaptive optics in vision science", Selected Topics in Quantum Electronics, IEEE Journal of, Volume: 10, Issue: 3,629- 635(2004).

[4] L. N. Thibos et al. "Standards for Reporting the Optical Aberrations of Eyes," Journal of Refractive Surgery, Sep-Oct, 18(5):s652-60(2002).

[5] JAMES C. WYANT and KATHERINE CREATH, "Applied Optics and Optical Engineering", Vol. XI, Academic Press, chapter 1, pp 39 (1992)